Angular distributions of neutron-nucleus collisions

Tapan Mukhopadhyay,* Joydev Lahiri,† and D. N. Basu‡
Variable Energy Cyclotron Centre, 1/AF Bidhan Nagar, Kolkata 700 064, India
(Received 10 March 2011; published 23 June 2011; corrected 29 June 2011)

We derive the total and the differential cross sections with respect to angle for neutron-induced reactions from an analytical model having a simple functional form to demonstrate the quantitative agreement with the measured cross sections. The energy dependence of the neutron-nucleus interaction cross sections are estimated successfully for energies ranging from 5 to 600 MeV. In this work, the effect of the imaginary part of the nuclear potential is treated more appropriately compared to our earlier work. The angular distributions for neutron scattering also agree reasonably well with the experimental data at forward angles.

DOI: 10.1103/PhysRevC.83.067603 PACS number(s): 24.10.−i, 25.40.−h, 28.20.Cz

The total and reaction cross sections of neutron-nucleus collisions for energies up to 600 MeV or more, are required in a number of fields of study in basic science [1,2] as well as many of applied nature [3–9]. Often, these cross sections are evaluated using phenomenological optical potentials, and much effort has gone into defining global sets of parameter values for those optical potentials with which to estimate cross sections as yet unmeasured. In this context it would be useful to study the systematics of neutron absorption and scattering cross sections on various nuclei well approximated by a simple convenient functional form [10,11]. The present model is an easy-to-use analytical parametrization that may be adequate to produce the scattering cross sections needed in Monte Carlo neutron transport calculations at energies higher than 150–200 MeV. It is worth noticing that the most important forward-scattering part of the angular distribution is reasonably described; however, the current model does not give a good accuracy for the whole angular range. Present results allow one to easily obtain good estimates of the total and inelastic cross sections from 5 to 600 MeV.

The optical potential for nuclear n-N interaction can be written as $-V - iW$ with V and W as positive quantities, and contains no Coulomb interaction. The phase shift δ in a WKB approximation is $[\int K'dr - \int k'dr]$ and the real part of it to a zeroth-order approximation [12] for a square well with radius R is $(K-k)R$, where K is the real part of K' and $k' = k$ is real due to absence of potential. The real wave numbers inside and outside the nucleus are, therefore, given by $K^2 = 2m(E+V)/\hbar^2$ and $k^2 = 2mE/\hbar^2$, respectively, where E is the incident neutron energy in the center-of-mass system and m is the reduced mass of the neutron-nucleus system. Hence β, which is two times the real part of the phase shift, is determined by the real potential V,

$$\beta = 2(K-k)R = 2\frac{(2m)^{\frac{1}{2}}}{\hbar}[\sqrt{E+V} - \sqrt{E}]R, \quad (1)$$

whereas the attenuation factor α is determined primarily by the imaginary potential W,

$$\alpha = e^{-\bar{R}/\lambda} = e^{-2mW\bar{R}/\hbar^2 K}, \quad (2)$$

where λ is the mean free path of the neutron inside the nucleus. The average chord length $\bar{R}$ of a neutron passing through a nucleus can be derived as

$$\bar{R} = \frac{\int_0^R 2\sqrt{R^2 - x^2}(I 2\pi x\, dx)}{\int_0^R I 2\pi x\, dx} = \frac{4}{3}R, \quad (3)$$

where I is the neutron flux that is the number of neutrons incident per unit area. Since $R \propto A^{\frac{1}{3}}$ $(R \sim r_0 A^{\frac{1}{3}})$, the above arguments imply that

$$\beta = \beta_0 A^{\frac{1}{3}}[\sqrt{E+V} - \sqrt{E}], \quad (4)$$

where $\beta_0 = \frac{2r_0(2m)^{\frac{1}{2}}}{\hbar}$ whose value is approximately 0.6, and the attenuation factor which is much less than unity but increases with energy (which is obvious from its expression) is given by

$$\alpha = \exp\left[-\alpha_0 r_0 A^{\frac{1}{3}} W/\sqrt{E+V}\right], \quad (5)$$

where $\alpha_0 = \frac{4(2m)^{\frac{1}{2}}}{3\hbar}$ whose value turns out to be 0.2929 and r_0 is the nuclear radius parameter. The first term $V_A = V_0 + V_1(1 - 2Z/A) + V_2/A$ of the real potential $V = V_A + V_E\sqrt{E}$ contains both the isoscalar and the isovector [13,14] components of the optical potential [15,16] where Z is the atomic number of the target nucleus, whereas the second term accounts for its energy dependence. The imaginary potential W is taken as $W = W_0 + W_E\sqrt{E+V}$ since the total kinetic energy of the neutron inside the nucleus with an attractive potential well of depth V is $E+V$. As the magnitude of the real part of the optical potential decreases with energy while the same for imaginary part increases, this implies that V_E is negative, whereas W_E is positive.

From partial-wave analysis of scattering theory, we know the standard expressions for scattering σ_{sc} and reaction σ_r cross sections as

$$\sigma_{sc} = \frac{\pi}{k^2}\sum_l (2l+1)|1-\eta_l|^2, \quad \sigma_r = \frac{\pi}{k^2}\sum_l (2l+1)[1-|\eta_l|^2],$$
$$\frac{d\sigma_{sc}}{d\Omega} = \frac{1}{4k^2}\left|\sum_l (2l+1)(1-\eta_l)P_l(\cos\theta)\right|^2, \quad (6)$$

*tkm@veccal.ernet.in
†joy@veccal.ernet.in
‡dnb@veccal.ernet.in

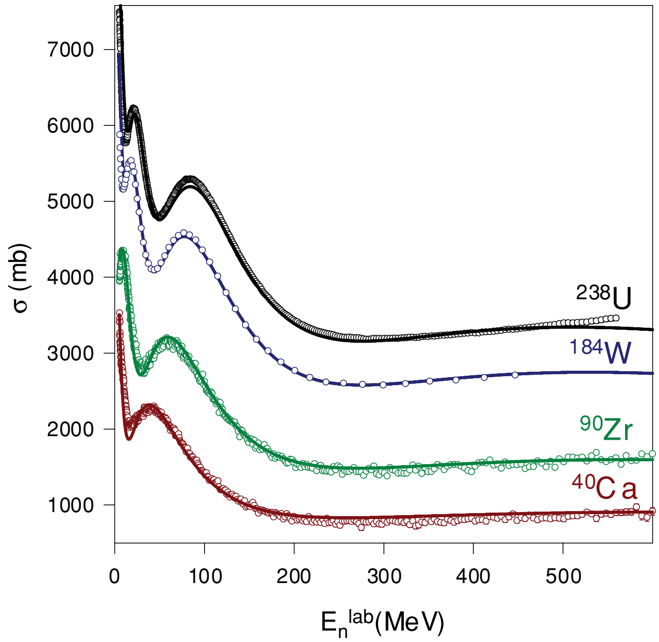

FIG. 1. (Color online) Total cross sections σ_{tot} vs incident neutron energies for ^{238}U, ^{184}W, ^{90}Zr, and ^{40}Ca target nuclei. The hollow circles represent the experimental data [20–22] for σ_{tot}, whereas the lines represent the same obtained theoretically with the present formulation which show good agreement with the measured cross sections.

where the quantity $\eta_l = e^{2i\delta_l}$, $P_l(\cos\theta)$ are the Legendre polynomials of order l, and θ is the scattering angle. With the assumption of the semiclassical optical model (or the so-called nuclear Ramsauer model) that the phase shift δ_l is independent of l and the summation over partial waves is performed up to the sharp cutoff kR_{ch} only, it follows that $\sigma_{\text{sc}} = \pi(R_{\text{ch}} + \lambdabar)^2(1 + \alpha^2 - 2\alpha\cos\beta)$ and $\sigma_r = \pi(R_{\text{ch}} + \lambdabar)^2(1 - \alpha^2)$ [17–19], where $\lambdabar = 1/k$, R_{ch} is the channel radius beyond which partial waves do not contribute, $\beta = 2\,\text{Re}\,\delta_l = 2\,\text{Re}\,\delta$, and $\alpha = e^{-2\,\text{Im}\,\delta_l} = e^{-2\,\text{Im}\,\delta}$; and summing over l from 0 to kR_{ch} yielded $\sum_{l=0}^{kR_{\text{ch}}}(2l+1) = (kR_{\text{ch}}+1)^2$. Thus

$$\sigma_{\text{tot}} = \sigma_{\text{sc}} + \sigma_r = 2\pi(R_{\text{ch}} + \lambdabar)^2(1 - \alpha\cos\beta),$$
$$\frac{d\sigma_{\text{sc}}}{d\Omega} = \frac{\lambdabar^2}{4}(1 + \alpha^2 - 2\alpha\cos\beta)\left[\sum_{l=0}^{kR_{\text{ch}}}(2l+1)P_l(\cos\theta)\right]^2. \tag{7}$$

The present model can be fitted to the experimental neutron total cross section σ_{tot}. The radius of the nuclear potential is given by $R = r_0 A^{\frac{1}{3}}$, whereas the channel radius can be parametrized as $R_{\text{ch}} = r_0 A^{\frac{1}{3}} + r_A\sqrt{E} + r_2$ with $r_A = r_{10}\ln A + r_{11}/\ln A$. The fits yield $r_{10} = -22.98 \times 10^{-3}$, $r_{11} = 10.27 \times 10^{-2}$, $r_2 = 23.22 \times 10^{-2}$, $V_0 = 46.51$, $V_1 = 6.74$, $V_2 = -117.52$, $V_E = -3.22$, and $\beta_0 = 0.5928$. These values are very close to or within the limit of the parameter values listed in Ref. [11]. The value of α_0 is kept fixed at 0.2929, and the nonlinear least-squares fits yield the value for the imaginary potential $W_0 = 5.293$ MeV and its energy dependence $W_E = 33.88 \times 10^{-2}$. The nuclear radius parameter r_0 is also fitted reasonably well to $1.378A^{\gamma}$ fm, which means that the nuclear potential radius $R = r_0' A^{\frac{1}{3}+\gamma}$ where $\gamma = 7.93 \times 10^{-3}$ is a very small number (needed for fine tuning) compared to $\frac{1}{3}$. In our earlier work [11] the effect of the imaginary potential was included in the parameter α in a somewhat *ad hoc* manner lacking justification for it to be weakly mass dependent. The present work is an improvement over our earlier work, since the imaginary part of the nuclear potential is now treated appropriately with the explicit appearance of the imaginary part of the nuclear potential. It is not that the predictions of the cross sections are greatly improved by the impact of these

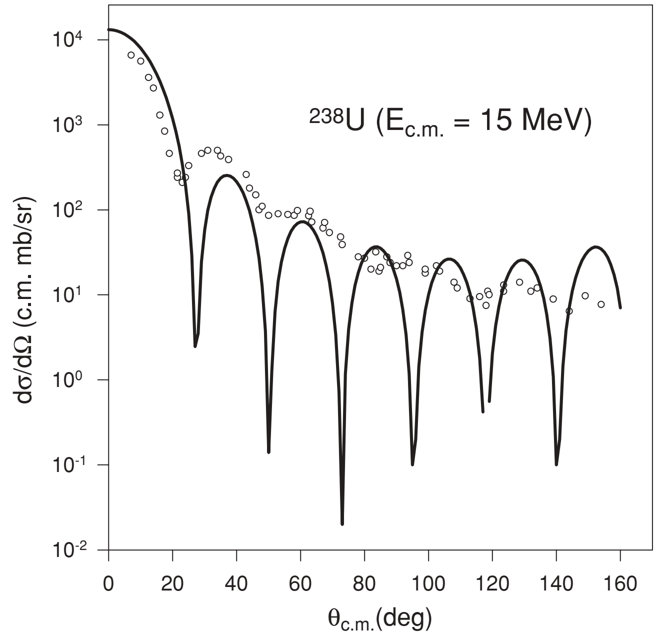

FIG. 2. (Color online) Theoretical (lines) and experimental (hollow circles) [23] angular distributions for neutron scattering for ^{238}U.

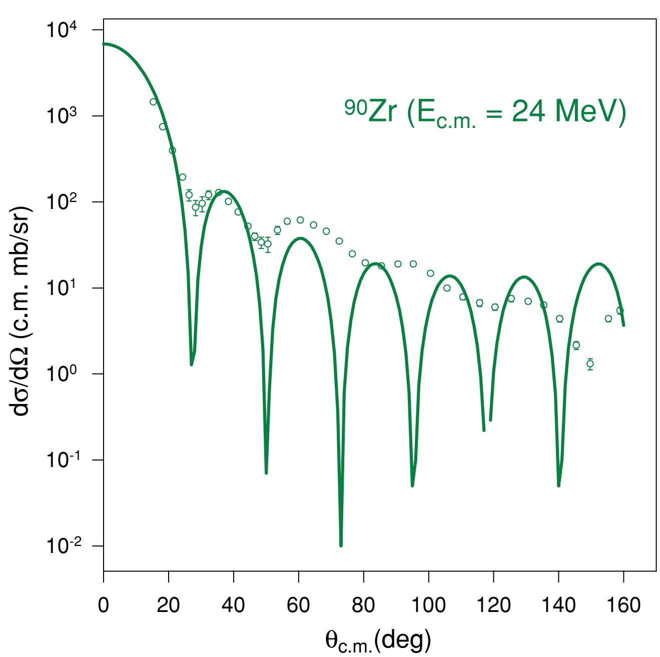

FIG. 3. (Color online) Same as Fig. 2, but for ^{90}Zr. The experimental data are from Ref. [24].

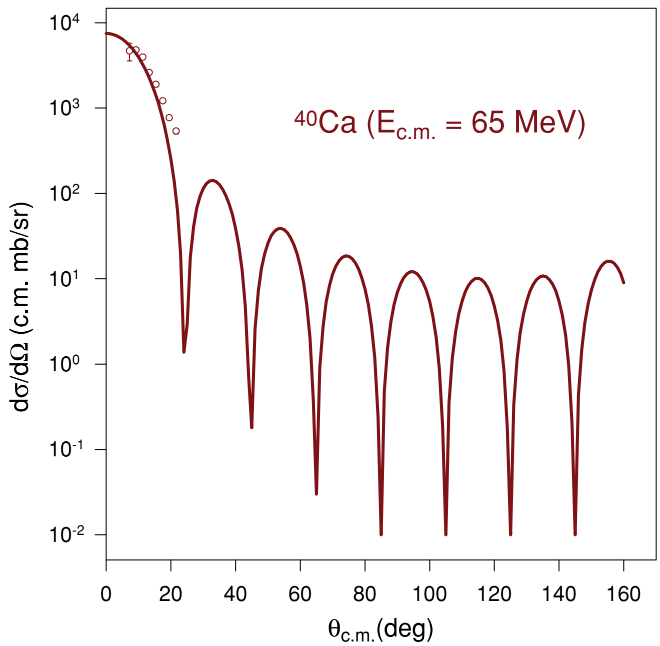

FIG. 4. (Color online) Same as Fig. 2, but for ^{40}Ca. The experimental data are from Ref. [25].

changes but that the present form of α, with imaginary potential appearing explicitly, has a profound theoretical basis.

Each calculation is performed at neutron incident energy intervals of 1 MeV and for various elements. The total cross sections (σ_{tot}) calculated with the present formalism show good agreement with the measured cross sections for the entire range of target nuclei. For illustration we show only four plots here. In Fig. 1, the variations of the total cross section σ_{tot} with incident neutron energy are plotted for ^{238}U, ^{184}W, ^{90}Zr, and ^{40}Ca target nuclei. The hollow circles represent the experimental data [20–22] for total cross sections σ_{tot}, whereas the lines represent the same obtained theoretically with present formulation which show good agreement with the measured cross sections. Figures 2–4 show the comparison of the theoretical and experimental [23–25] angular distributions for neutron scattering for different target nuclei in the center-of-mass (c.m.) system. The present model also compares favorably with the optical model calculations [25] for the forward maximum (0°–25°) in the elastic scattering distribution. This is not surprising, since the present model which fits the total neutron cross section quite accurately (within a few percent) predicts the zero-degree elastic cross section which relates the zero-degree cross section to the total cross section (imaginary part of the forward-scattering amplitude [$\mathrm{Im}\, f(0°) = \frac{k\sigma_{tot}}{4\pi}$]. The average elastic cross section is also well described (to a few percent) by the present semiclassical optical model, since the model is able to fit the oscillations in the total cross section to the order of a few percent and these oscillations are due to variations in the elastic cross section. However, beyond 30°, there are large discrepancies in the angular distributions between the calculated and the measured values.

In summary, we constructed an analytical model, justified it from the optical model and nuclear reaction theory approach, and applied it to derive the systematics and performed calculations of neutron-nucleus total cross section, the scattering cross section, and the reaction cross section, and we then estimated these cross sections for a wide range of target nuclei. The extracted parameters for the present analytical model provide global fits to the neutron total cross sections spanning quite a large number of nuclei. The angular distribution is also well estimated at forward angles (0°–30°). We conclude that the present estimates of neutron scattering cross sections are very important for the reactor physics calculations [3–9] of the Accelerator Driven Sub-critical Systems (ADSS) applications. The neutron-nucleus reaction cross sections are very useful for the theoretical calculations of radioactive ion beam [1,2] production or for performing Hauser-Feshbach [26] calculations with Monte Carlo simulations [27] to estimate the cross sections for neutron-induced fission and neutron multiplicities [28], and they may serve as inputs to intranuclear cascade codes such as the MCNPX package. Although the simple semiclassical optical model obtained to calculate total cross sections up to 600 MeV are very useful and almost as accurate as the phenomenological optical model potentials which are limited to 150–200 MeV, the results for the angular distributions (differential cross sections) agree reasonably with the experimental data only at forward angles below 30°, implying that they are expected to be more accurate for optical model calculations.

[1] W. T. Diamond, Nucl. Instrum. Methods Phys. Res. Sect. A **432**, 471 (1999).
[2] S. Essabaa *et al.*, Nucl. Instrum. Methods Phys. Res. Sect. B **204**, 780 (2003).
[3] A. Boudard *et al.*, Nucl. Phys. A **663**, 1061 (2000).
[4] C. H. M. Broeders and I. Broeders, Nucl. Eng. Des. **202**, 209 (2000).
[5] I. Demirkol *et al.*, Nucl. Sci. Eng. **147**, 83 (2004).
[6] A. Kaplan *et al.*, Appl. Radiat. Isot. **67**, 570 (2009).
[7] H. Yapýcý *et al.*, Ann. Nucl. Energy **34**(5), 374 (2007).
[8] I. Demirkol *et al.*, Chin. J. Phys. **46**(2), 124 (2008).
[9] C. Rubbia *et al.*, CERN Rep. CERN/AT/95-44 (ET), 1995 (unpublished).
[10] P. K. Deb and K. Amos, Phys. Rev. C **69**, 064608 (2004); P. K. Deb, K. Amos, and S. Karataglidis, *ibid.* **70**, 057601 (2004).
[11] T. Mukhopadhyay, J. Lahiri, and D. N. Basu, Phys. Rev. C **82**, 044613 (2010); **83**, 039902(E) (2011).
[12] C. B. O. Mohr, Aust. J. Phys. **10**, 110 (1957).
[13] A. M. Lane, Nucl. Phys. **35**, 676 (1962).
[14] G. R. Satchler, *Direct Nuclear Reactions*, International Series of Monographs on Physics (Oxford University, Oxford, 1983), p. 471.
[15] C. R. Gould *et al.*, Phys. Rev. Lett. **57**, 2371 (1986).
[16] J. D. Anderson and S. M. Grimes, Phys. Rev. C **41**, 2904 (1990).
[17] I. Angeli and J. Csikai, Nucl. Phys. A **158**, 389 (1970).
[18] I. Angeli and J. Csikai, Nucl. Phys. A **170**, 577 (1971).
[19] I. Angeli, J. Csikai, and P. Nagy, Nucl. Sci. Eng. **55**, 418 (1974).
[20] R. W. Finlay, W. P. Abfalterer, G. Fink, E. Montei, T. Adami, P. W. Lisowski, G. L. Morgan, and R. C. Haight, Phys. Rev. C **47**, 237 (1993).

[21] W. P. Abfalterer, F. B. Bateman, F. S. Dietrich, R. W. Finlay, R. C. Haight, and G. L. Morgan, Phys. Rev. C **63**, 044608 (2001).
[22] F. S. Dietrich *et al.*, Phys. Rev. C **67**, 044606 (2003).
[23] B. Ya. Guzhovskiy, J. Atomnaya Energiya **11**, 395 (1961).
[24] Y. Wang and J. Rapaport, Nucl. Phys. A **517**, 301 (1990).
[25] J. H. Osborne *et al.*, Phys. Rev. C **70**, 054613 (2004).
[26] W. Hauser and H. Feshbach, Phys. Rev. **87**, 366 (1952).
[27] Projection Angular momentum Coupled Evaporation code [PACE2].
[28] T. Mukhopadhyay and D. N. Basu, Phys. Rev. C **76**, 064610 (2007); **79**, 017602 (2009).